Exploring the Origin of Fragile-to-Strong Transition in Some Glass-Forming Liquids

Yue, Yuanzheng; Hu, L. N.

Published in:
Fragility of Glass-Forming Liquids

Publication date:
2014

Document Version
Publisher's PDF, also known as Version of record

13

Exploring the Origin of Fragile-to-Strong Transition in Some Glass-Forming Liquids

Yuanzheng Yue and Lina Hu

The slow dynamics of glass-forming liquids is a complex subject of the condensed matter science. But the fragile-to-strong transition, which was observed not long ago [Ito, et al, Nature 1999], makes this subject even more complex since it is extremely challenging to directly probe the structural, topological and thermodynamic changes causing this transition. The theory for describing the transition has not been fully established. In this paper, we summarize our current understanding of the fragile-to-strong transition in some glass-forming liquids based on our two published papers and recent unpublished results. At the same time we point out major challenges and perspectives for clarifying both the origin and consequences of the fragile-to-strong transition.

13.1 Introduction

Since Angell proposed the key dynamical concept - liquid fragility three decades ago [1], scientists from different fields have been exploring the origin and consequences of liquid fragility in terms of structure, topology, and thermodynamics. It is inspiring that substantial progress in understanding of liquid fragility has been made over the past three decades with respect to a large range of glass forming liquids. However, while old crucial glass problems have been clarified, new challenging problems have merged. One of these challenging problems is about the origin of the fragile-to-strong (F-S) transition observed in many glass forming systems such as water [2] and metallic systems [3, 4]. A big hurdle for

tackling this problem is the difficulty in directly probing the structural, dynamical and thermodynamic evolvements in the F-S transition temperature region since it occurs right within 'n-man'land, at least for most of the F-S transition liquids, where dynamic measurements are hindered by crystallization. Despite the obstacle, scientists have still made advances in investigating the F-S transition by applying indirect approaches. In the present contribution, we summarize our recent findings and new insights into the F-S transition problem based on our two published papers [4, 5] and very recent results [6, 7, 8].

13.2 Fragile-to-strong Transition as a Universal Feature of Strong Liquids

In ref. [4], we observed a striking fragile-to-strong transition in all the metallic glass-forming liquids (MGFLs) that we have studied. The extent of the fragile-to-strong transition depends on the chemical composition of MGFLs. These observations along with our follow-up work suggest that the F-S transition be a general dynamic feature of MGFLs. The extent of the F-S transition depends on the chemical composition, and may be quantified by a new parameter $f = m_{fragile}/m_{strong}$, where $m_{fragile}$ and m_{strong} are the fragility indices of the fragile and strong phases, respectively. However, the detailed dynamic trend of the MGFLs cannot be described by the existing three-parameter viscosity models. In this context we proposed a new model to describe the F-S transition of MGFLs [4] and we expect that it may be extended to other liquids showing the F-S transition. This model contains a strong term and a fragile term, which are correlated with two dynamically competing phases, and hence two relaxation mechanisms, respectively. Our findings indicate that the F-S transition is intrinsic to strong liquid systems as a relaxation mode of higher entropy and higher activation barrier becomes dominant at some high temperatures for these systems. The size evolvement of the medium range ordered clusters in these systems upon cooling from liquidus temperatures towards glass transition temperatures is non-monotonic and experiences an abrupt change when crossing the F-S transition region. Thermodynamically, the F-S transition is accompanied by a Lambda transition [9].

13.3 Origin of the Fragile-to-strong Transition

In ref. [5], we studied the influence of the cooling rate on the sub-T_g enthalpy relaxation behavior for two kinds of metallic glass ribbons. Remarkably, we observed an abnormal three-step relaxation pattern with respect to the cooling rate dependence of the activation energy of enthalpy relaxation in the hyperquenched (HQ) ribbons. We regard this abnormal sub-T_g relaxation behavior as a thermodynamic signature of the F-S transition due to the competition between the low and high temperature clusters in MGFLs. Based on our recent

results [6, 7], this abnormal sub-T_g relaxation behavior might be a general feature of the hyperquenched metallic glasses, and its origin is closely related to the chemical and/or structural heterogeneity in supercooled liquids. Through this work, the hyperquenching-annealing strategy is proven to be a useful tool for providing insights into the thermodynamic source of the F-S transition.

In ref. [7], we observed a pronounced abnormal calorimetric response in the HQ LaAlCuNi glass ribbons fabricated at different cooling rates. We found that there is a critical intermediate regime of fabrication cooling rates (corresponding to the rotation speed of about 2000 round/min), where both enthalpy relaxation and crystallization behaviors greatly differ from those of glasses formed at other cooling rates. This abnormal behavior corresponds well with the pressure-induced relaxation anomaly in the same glass. The fictive temperature of the glass ribbons formed at 2000 r/min is close to that determined by both the kinetic methods and the molecular simulations for the F-S transition. The abnormal relaxation behavior indicates that the thermodynamic F-S transition indeed occurs in MGFLs. To further explore the structural origin of the F-S transition we analyzed the microstructural evolutions during the F-S transition in a LaAlCuNi liquid [8]. Very recently, by performing viscosity and heat capacity measurements we found that the first-order liquid-liquid transition occurs in a CuZrAl liquid series even above the liquidus temperature. This transition is also observed in other metallic systems [9]. Such results give implications for the existence and competition of both strong and fragile phases.

13.4 Challenges and Perspective

It is speculated that the F-S transition might be attributed to the destruction of medium-range isocahedral order in the melt with increasing temperature. However, direct experimental evidence is missing, and hence we are far from complete understanding of the F-S transition. This is mainly hindered by the limitation of existing experimental approaches for accessing the no-man'land. To reveal the origin of the F-S transition we must find a way to directly probe both structural changes in microscopic length scales and fluctuation in density. However, two recent attempts in probing the dynamic and thermodynamic response of the F-S transition seem promising [5, 6, 7, 9, 10]. The first one is to trap the potential energy state and structure of metallic liquids in the low temperature regime of the F-S transition by hyperquenching, and subsequently to partially anneal HQ samples below T_g and afterwards upscan them in a calorimeter and conduct structural characterizations. By controlling hyperquenching, annealing and calorimetric protocols, we will be able to access the relaxation modes and structural changes and hence infer the microscopic origin of the F-S transition in a certain range of fictive temperatures. The second one is to dive into the supercooled region as deep as possible by using containerless levitation melting techniques, and simultaneously to directly access the dynamic (e.g. relaxation time or viscosity), thermodynamic (e.g. density) and

structural evolvement of the supercooled liquids during the F-S transition by means of newly developed *in situ* characterization techniques [10].

The lower temperature limit of the supercooled liquid region is getting lower with rapid development of the levitation melting technology, whereas the upper limit of the fictive temperature becomes higher with development of hyperquenching technology. In this case, non-man'land is gradually being occupied. However, on the other hand, there is still some non-man'land remaining, i.e., the gap between the upper and lower limit is not fully closed yet, and hence dynamic and thermodynamic data in the middle range of the F-S transition cannot be directly obtained. Thus, the viscosity versus temperature trend can be only approximately achieved if fitting the available data to Eq. (7) in [4]. Despite the difficulty in further narrowing the non-man'land, we are optimistic about major progress for the following reasons.

First, technologically it will be possible to drastically raise hyperquenching rate (e.g., $10^8 K/s$) for arresting the structure and the high potential energy state of the glass-forming liquids exhibiting the F-S transition. By doing so, we can achieve the fictive temperatures that covers the F-S transition region as much as possible. A drastic increase of hyperquenching rate could be realized by fabricating low dimensional glassy materials such as nano-fibers and -films. Thus, the structure and enthalpy relaxation of these high T_f glasses can be determined under ambient conditions, and hence the details of the dynamics can be inferred. This enables accessing the higher part of the potential energy landscape, and acquiring information on configurationally and vibrationally excited states in glass by means of sub-T_g annealing, subsequent calorimetric scanning, and other advanced characterization techniques. To capture the thermodynamic signature of the F-S transition, both conventional and flash differential scanning calorimeters should be applied. Furthermore, understanding of structural and dynamic heterogeneities will constitute a basis for understanding the F-S transition. Recently we succeeded in detecting the structural heterogeneity by performing the sub-T_g enthalpy relaxation and atomic resolution transmission electron microscopy [11].

Second, it will also be possible for a glass forming liquid to enter deeply no-man'land by applying the improved containerless levitation technique. For example, scientists have recently succeeded in driving the liquid alumina down to the temperature 400 K below the liquidus temperature without crystallizing, while viscosity and density were simultaneously measured [10]. It would be highly interesting if we could conduct *in-situ* structural characterizations on this kind of liquid as done on the MGFLs [10]. Actually, there has already been a sign that the liquid alumina looks like metallic liquids in terms of the F-S transition. Recently, the dynamics of the binary alumina-calcium series is being probed. Moreover, the liquid-liquid phase relations have been directly observed in levitated yttria-alumina drops with X-rays and high speed imaging [12]. With further improvement of the levitation-in situ characterization techniques, we expect that it would be possible to directly probe the density transition

of the liquid and the abrupt change in cluster structure and size in the F-S transition regime.

Finally, the molecular dynamic simulation and advanced theoretical approaches will be highly valuable for revealing the origin of the F-S transition. It would be a big step forward if one can model the abnormal evolvement of cluster structure in the liquids during the F-S transition, which greatly deviates from the evolving trend of the cooperative rearranging regions predicted by the Adam-Gibbs model.

References

[1] C. A. Angell, in Relaxations in Complex Systems, ed. K. Ngai and G.B. Wright, National Technical Information Service, U.S. Department of Commerce, Springfield, VA 22161 (1985), p. 1.

[2] K. Ito, C. T. Moynihan, and C. A. Angell, "thermodynamic connection to the fragility of glass-forming liquids" *Nature* **398**, 492, 1999.

[3] C. Way, P. Wadhwa, and R. Busch, "The influence of shear rate and temperature on the viscosity and fragility of the $Zr_{41.2}Ti_{13.8}Cu_{12.5}$ $Ni_{10.0}Be_{22.5}$ metallic-glass-forming liquid" *Acta Mater.* **55**, 2977, 2007.

[4] C. Z. Zhang, L. N. Hu, Y. Z. Yue and J. C. Mauro, "Fragile-to-strong transition in metallic glass-forming liquids", *J. Chem. Phys.* **133**, 014508, 2010.

[5] L. N. Hu, C. Zhou, C. Z. Zhang and Y. Z. Yue, "Thermodynamic anomaly of the sub-T_g relaxation in hyperquenched metallic glasses" *J. Chem. Phys.* **138**, 174508, 2013.

[6] L. N. Hu, Y. Z. Yue and C. Z. Zhang, "Normal sub-T_g enthalpy relaxation in the CuZrAl metallic glasses far from equilibrium" *Appl. Phys. Lett.* **98**, 081904, 2011.

[7] X. N. Yang, L.N. Hu, C. Zhou, C. Z. Wang, J. C. Mauro and Y. Z. Yue, "Thermodynamic study of the fragile-to-strong transition in metallic glass-forming liquids" *J. Chem. Phys.* To be published.

[8] C. Zhou, L. Hu, J. Y. Qin, Q. J. Sun, Y. Z. Yue, "Indication of liquid-liquid phase transition in CuZr-based melts" *Appl. Phys. Lett.* 103 (2013) 171–904.

[9] S. Wei, F. Yang, J. Bednarcik, I. Kaban, O. Shuleshova, A. Meyer, R. Busch, "Liquid-liquid transition in a strong bulk metallic glass-forming liquid" *Nature Comm.* **4**, 2083, 2013.

[10] N. Greaves et al. Unpublished data (2013).

[11] Y. F. Zhang, G. Yang and Y. Z. Yue, "Calorimetric signature of structural heterogeneity in a ternary silicate glass" *J. Am. Ceram. Soc.* 96 (2013) 3035–3037.

[12] G. N. Greaves, M. C. Wilding, S. Fearn, D. Langstaff, F. Kargl, S. Cox, Q. Vu Van, O. Majrus, C. J. Benmore, R. Weber, C. M. Martin, L. Hennet, "Detection of first order liquid-liquid phase transitions in yttrium oxide luminium oxide melts" *Science* **322**, 566 (2008).

Reprint 13-1: Fragile-to-strong Transition in Metallic Glass-forming Liquids

C. Zhang, L. Hu, Y. Yue and J. C. Mauro

J. Chem. Phys., 133, 041508 (2010)

Fragile-to-strong transition in metallic glass-forming liquids

Chunzhi Zhang,[1] Lina Hu,[1] Yuanzheng Yue,[1,2,a)] and John C. Mauro[3]
[1]*Key Laboratory for Liquid-Solid Structural Evolution & Processing of Materials, Shandong University, Jinan 250061, China*
[2]*Section of Chemistry, Aalborg University, DK-9000 Aalborg, Denmark*
[3]*Science and Technology Division, Corning Incorporated, Corning, New York, USA*

(Received 11 February 2010; accepted 4 June 2010; published online 7 July 2010)

Two of the Earth's most abundant substances, water and silica, exhibit some of the most unusual properties in nature. Among these is an anomalous scaling of liquid dynamics, which appear non-Arrhenius (or "fragile") at high temperatures yet Arrhenius (or "strong") at low temperatures. Here we show that this fragile-to-strong (F-S) transition is not limited to a few liquids such as water and silica, but is possibly a general behavior of metallic glass-forming liquids. We also propose a general model for the viscosity of F-S liquids that captures the scaling of dynamics across both the fragile and strong regimes. © *2010 American Institute of Physics*. [doi:10.1063/1.3457670]

I. INTRODUCTION

As a liquid is supercooled through the glass transition region, the viscosity increases by more than twelve orders in magnitude. This slowing-down process is characterized by the concept of liquid fragility.[1–4] Upon supercooling toward the glass transition temperature, T_g, in some liquids the equilibrium viscosity increases in an Arrhenius-like fashion (strong liquids), but in others the viscosity displays highly non-Arrhenius scaling (fragile liquids). According to the standard definition,[1–4] the fragility index m is given by

$$m = \left.\frac{d \log_{10} \eta}{d(T_g/T)}\right|_{T=T_g}, \tag{1}$$

where η is shear viscosity and T is the absolute temperature. The concept of liquid fragility is widely recognized as one of the most intriguing topics in modern glass physics.

The equilibrium viscosity of a glass-forming liquid can be described by the Mauro–Yue–Ellison–Gupta–Allan (MYEGA) equation[5]

$$\log \eta = \log \eta_\infty + \frac{B}{T}\exp\left(\frac{C}{T}\right), \tag{2}$$

where η_∞ is the viscosity in the high temperature limit and B and C are constants related to the onset of rigidity in the liquid network.[5] These parameters are typically obtained by fitting the experimental viscosity data to Eq. (2). It has been shown that Eq. (2) provides better fits to measured viscosity data compared to previous models such as Vogel–Fulcher–Tammann and Avramov–Milchev.[5] The fragility parameter m, can be derived from Eqs. (1) and (2) as[5]

$$m = \frac{B}{T_g}\left(1 + \frac{C}{T_g}\right)\exp\left(\frac{C}{T_g}\right), \tag{3}$$

where T_g is the standard glass transition temperature.[5] Alternatively, one can determine the parameters B, C, and hence m using a calorimetric method[6–8] based on the dependence of the fictive temperature T_f on the heating rate ϕ near the glass transition. With this approach, Eq. (2) is expressed as

$$\log \phi = \log \phi_\infty - \frac{B}{T_f}\exp\left(\frac{C}{T_f}\right), \tag{4}$$

where ϕ_∞ is the heating rate in the limit of infinite fictive temperature. The value of m calculated by this method is consistent with that obtained by the standard kinetic method.[6]

For most glass-forming liquids, a single fragility parameter at T_g is sufficient to describe equilibrium dynamics across the full range of temperatures. However, certain glass-formers such as water and silica require two different fragility parameters to reflect the changing fragility of those liquids in different temperature regimes. In other words, an initially fragile liquid is transformed into a strong liquid upon supercooling toward T_g. This is the so-called fragile-to-strong (F-S) transition, first discovered in water by Ito *et al.*[9] Water is one of the most fragile of any liquids at temperatures above the liquidus, T_{liq}. However, it is one of the strongest near the glass transition.[1,10] Kinetically speaking, the temperature dependence of the α relaxation time for water changes from a pronounced non-Arrhenius to a nearly Arrhenius behavior in the temperature range of 225–230 K.

To clarify the origin of the F-S transition, numerous studies have been carried out both theoretically and experimentally. Jagla[11] proposed a useful model that ascribes the F-S transition in water to a competition between two different local structures. In terms of Tanaka's two-order-parameter model[12] of tetrahedral liquids, the F-S transition of water can be interpreted as the crossover from a non-glass-forming to a glass-forming branch. Liu *et al.*[13] attribute the F-S transition to a translation from a high-density liquid to a low-density liquid. Finally, Hedström *et al.*[14] suggest that the F-S transition in water is a result of merging of a nonobservable α relaxation and a local β relaxation.

Besides water, the fragile-to-strong transition is also found in SiO_2 (Refs. 15 and 16) and in BeF_2.[17] Analysis of

a)Electronic mail: yy@bio.aau.dk.

TABLE I. Optimized viscosity parameters of Eq. (2), expressed in terms of the glass transition temperature T_g, the fragility parameters m and m', and the F-S transition magnitude $f=m'/m$.

Composition	$\log \eta_\infty$ (Pa s)	T_g (K)	m'	m	f
$Gd_{55}Al_{25}Co_{20}$	−2.65	589	113	25	4.5
$Gd_{55}Al_{25}Ni_{10}Co_{10}$	−2.58	579	133	25	5.3
$Pr_{55}Ni_{25}Al_{20}$	−3.05	484	156	19	8.2
$Sm_{55}Al_{25}Co_{10}Ni_{10}$	−2.33	551	130	37	3.5
$Sm_{50}Al_{30}Co_{20}$	−2.40	586	136	29	4.7
$Sm_{55}Al_{25}Co_{10}Cu_{10}$	−2.71	534	114	27	4.2
$La_{55}Al_{25}Ni_{20}$	−3.03	491	127	40	3.2
$La_{55}Al_{25}Ni_{15}Cu_5$	−3.23	474	130	34	3.8
$La_{55}Al_{25}Ni_5Cu_{15}$	−3.27	459	134	40	3.4
$Al_{87}Co_8Ce_5$	−2.72	559	114	34	3.3
$Ce_{55}Al_{45}$	−3.12	541	127	32	4.0
Water	−3.90	165	98	22	4.5

experimental and simulation data shows that liquid silica, which is an archetypical strong liquid near T_g, may be transformed into a fragile liquid at temperatures above roughly 3300 K.[18] Simulations of the silica energy landscape have revealed that the F-S transition is related to the polyamorphic behavior of silica glass.[19]

While in the previous literature most MGFLs are characterized as relatively strong liquids (stronger than most oxides), recently the fragility of supercooled $Zr_{41.2}Ti_{13.8}Cu_{12.5}Ni_{10.0}Be_{22.5}$ was found to differ from that of the equilibrium liquid at high temperatures.[20] This implies that a possible F-S transition might occur in this specific system. In order to find out whether the F-S transition is a general feature of metallic glass-forming liquids (MGFLs), we perform a thorough experimental study of the dynamical behavior of eleven MGFLs (see Table I) over both the high and low temperature regimes. At the same time, we attempt to establish a model for the viscosity of F-S liquids that captures the scaling of dynamics across both the fragile and strong regimes. This model should also be capable of describing the viscosity of the non-F-S liquids.

II. EXPERIMENTAL PROCEDURE

The samples for viscosity and T_g measurements were prepared from a mixture of pure elements by arc melting under an argon atmosphere. Then the pre-alloyed ingots were remelted in a high-frequency induction furnace and rapidly solidified into continuous ribbons by the single roller melt-spinning technique. The glassy ribbons were obtained by the melt-spinning technique.

The low temperature viscosities of the Ce-, Al-, Gd-, Sm-, and La-based glassy ribbons were measured by means of a calorimetric method described elsewhere.[6–8] The calorimetric measurements were performed using a differential scanning calorimeter (DSC) with a the sample mass of 20 ± 0.5 mg. All DSC measurements were conducted in a flowing (30 cm^3/min) nitrogen gas. The temperature error was ±2 K. The samples underwent two runs of DSC up- and downscans. The rate of each upscan was always equal to that of the prior downscan. The upscan rate ranges from 1 to 50 K/min. The DSC output (heat flow) of the first upscan reflects the enthalpy response of a fresh sample with an unknown thermal history (i.e., an unknown cooling rate that the sample experiences during melt-spinning), whereas that of the second upscan reflects the enthalpy response of the sample with a well defined thermal history (i.e., a known cooling rate). The onset temperature of the endothermic jump at the second upscan was assigned as the calorimetric fictive temperature, T_f.[21] The T_f value increases with increasing the upscan rate equal to the prior downscan rate, as shown in Eq. (4). The T_f value measured during an upscan at 20 K/min after a previous downscan at the same rate gives the standard glass transition temperature, T_g. According to previous studies,[6–8] the fictive temperature dependence of the reciprocal DSC upscan rate corresponds to the temperature dependence of the equilibrium viscosity. This ensures that the data shown in the supercooled liquid around T_g in Figs. 1–4 reflect the equilibrium values of viscosity, rather than the nonequilibrium or "isostructural" viscosity of the glass.[22,23] The low-temperature viscosities of Pr-based metallic samples were measured using the three-point beam bending method described in detail elsewhere.[24]

High-temperature viscosity measurements were carried

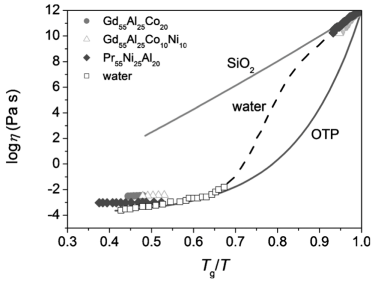

FIG. 1. Viscosities (η) of liquid water and three metallic glass-forming liquids as a function of the T_g scaled temperature T, where T_g is the glass transition temperature. The dashed line shows a sketch of the F-S transition region for water. The solid lines are fits of Eq. (2) to the experimental viscosity data of SiO_2 and OTP.

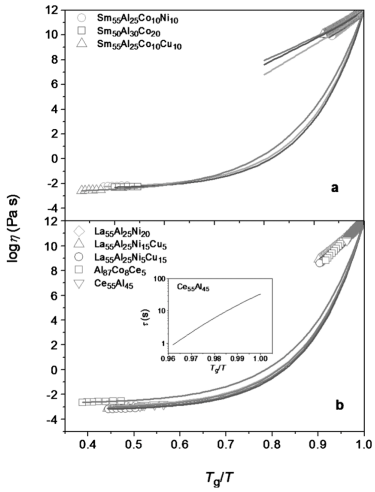

FIG. 2. Viscosities (η) as functions of the T_g scaled temperature T for eight metallic glass-forming liquids. Solid curves: fits of Eq. (2) to the measured viscosity data. Inset in Fig. 2(b): the relaxation time as a function of T_g/T for the $Ce_{55}Al_{45}$ glass.

out in a high vacuum atmosphere with an oscillating viscometer.[25] The samples were placed in a vessel hung by a torsional suspension wire. The vessel was set to oscillate about a vertical axis, and the resulting motion was gradually damped due to frictional energy absorption and dissipation within the melt. The samples sealed in a vacuum of 10^{-3} Torr were overheated to 250 K above liquidus temperatures and held at the temperature for 30 min. Then the samples were cooled to the detected temperature and held for 30 min before the viscosity measurement. At each temperature the viscosity was measured three times. Above the liquidus temperature, the relaxation time is so short that the measured data directly represent the equilibrium values of viscosity.

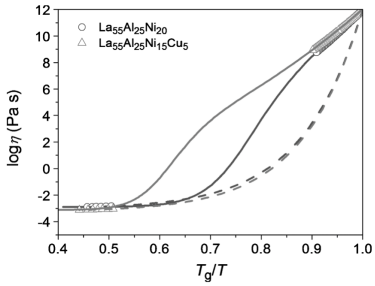

FIG. 3. Comparison of the models in Eq. (2) (dashed lines) and Eq. (7) (solid lines). Here, Eq. (2) is fit to the high temperature viscosity data only. The viscosity data are shown for two metallic glass-forming liquids.

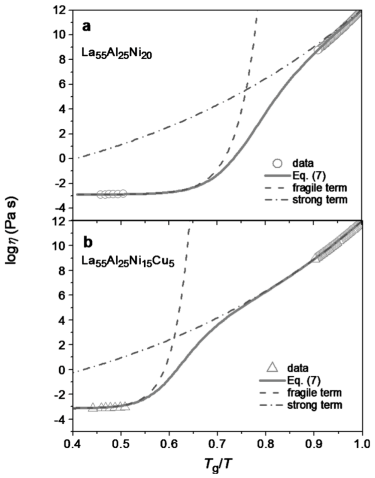

FIG. 4. The double exponential form of Eq. (7) includes two contributions to the overall viscous behavior of metallic glass-forming liquids: a fragile term dominant at high temperatures and a strong term dominant at low temperatures. These terms correspond to two different relaxation mechanisms, which have a comparable time scale during the F-S transition. The fits are shown for two metallic glass-forming liquids: (a) $La_{55}Al_{25}Ni_{20}$; (b) $La_{55}Al_{25}Ni_{15}Cu_5$.

III. RESULTS

Figure 1 shows the fragility diagram for three MGFLs: $Gd_{55}Al_{25}Co_{20}$, $Gd_{55}Al_{25}Co_{10}Ni_{10}$, and $Pr_{55}Ni_{25}Al_{20}$.[26–28] The viscosity data for SiO_2, orthoterphenyl (OTP), and water are also presented for comparison. The high temperature viscosities of the MGFLs were measured using the oscillation vessel method. The viscosity data of the Gd-based glass samples were measured using the calorimetric method while those of the Pr-based using the three-point beam bending method. Near T_g the fragility, i.e., the slope of the $\log \eta \sim T_g/T$ curves [see Eq. (1)], of the metallic glasses is close to that of SiO_2 and water, but significantly smaller than that of OTP. This indicates that the low T supercooled liquids are relatively strong. In contrast, on the high T side (above T_{liq}), the fragility of the MGFLs is close to that of OTP and water. This indicates that the MGFLs at high T are rather fragile. Over the entire range of temperatures, there is a remarkable similarity in the dynamical behavior of MGFLs and water. Figure 2 shows the fragility diagram for eight additional MGFLs, all of which exhibit a pronounced F-S transition similar to that in water.

The viscosity data shown in Fig. 2 were obtained for three Sm-based bulk alloys, three La-based bulk alloys,[6,27] one Ce-based alloy ($Ce_{55}Al_{45}$), and one marginal alloy ($Al_{87}Co_8Ce_5$) (Refs. 21 and 28) for both the equilibrium liquid above T_{liq} and the supercooled liquid near T_g. The high and low temperature viscosity data are independently fit to Eq. (2). The high temperature viscosity data were measured using the oscillation vessel method while the low tempera-

ture viscosity data were obtained using the calorimetric approach. The two kinds of fitting curves are extrapolated to a common T_g point as indicated in Fig. 2. The extent of the F-S transition of the eight liquid metals varies only slightly from each other and is similar to that observed in water. In the inset of Fig. 2(b), the structural relaxation time τ is plotted against the T_g-scaled temperature for the $Ce_{55}Al_{45}$ glass during heating. The structural relaxation time τ is determined using the Maxwell equation $\tau = \eta/G_\infty$, where G_∞ is the shear modulus at infinite frequency. From this representative plot, it is confirmed that the low temperature viscosities shown in this work are indeed characteristic of the supercooled liquid region near T_g.

To quantify the extent of the F-S transition in the chosen MGFLs, we perform two steps of data fitting. In the first step, the low temperature (near T_g) viscosity data are fit to Eq. (2) to obtain a set of parameters such as B and C, from which the fragility parameter m is calculated using Eq. (3). The parameter m quantifies the fragility of the supercooled liquids near T_g. In the second step, the high temperature ($>T_{liq}$) viscosity data, together with the fixed data point of 10^{12} Pa s at T_g,[3,22] are fit to Eq. (2) to get another set of parameters (B' and C'), from which the fragility parameter m' is obtained using Eq. (3). The parameter m' quantifies the fragility of the liquids above T_{liq}. For a liquid without F-S transition, m and m' have the same value. However, for a liquid with a F-S transition, m and m' will have different values, i.e., $m < m'$. The difference in fragility between the equilibrium and the supercooled liquids can be quantified by the ratio m'/m. Here, this ratio is referred to as the F-S transition factor f, i.e.,

$$f = \frac{m'}{m} \geq 1, \tag{5}$$

which we propose as a quantitative measure for the extent of the F-S transition. The larger the factor f, the larger is the extent of the F-S transition during cooling. The definition of f is especially important since the F-S transition itself is not directly detectable during a normal (i.e., slow) cooling procedure, since these liquids—both water and MGFLs—are highly unstable in the F-S transition region due to the intervention of crystallization. To obtain viscosity data near T_g, the liquid must be rapidly quenched, in some cases, hyperquenched (cooling rate $>10^5$ K/s) to become a glass, depending on the specific glass-forming ability of MGFLs. Then, the viscosities of the reheated glass are measured in the temperature range between T_g and the onset temperature of crystallization.

Table I lists the values of log η_∞, T_g, m, and m', and the F-S transition factor $f = m'/m$, for all of the liquids under study. The F-S transition parameter f is larger than 1 and ranges from 3.2 to 8.2 for these liquids. The extent of the F-S transition differs from one metallic liquid to another, with $Pr_{55}Ni_{25}Al_{20}$ having the largest of all studied MGFLs. It should be mentioned that the differences in experimental methods for measuring the viscosity data in the supercooled liquid region near T_g could cause a scattering of the f values.[29] However, such scattering is much smaller than the extent of the F-S transition itself.

IV. DISCUSSION

The factor f listed in Table I confirms the existence of a F-S transition in the studied MGFLs. Such a transition might be a general dynamic behavior of metallic glass-forming liquids. While the factor f provides a means for quantifying the extent of the F-S transition, it is based on separate fits of a three-parameter viscosity model to the high and low temperature regimes, neither of which captures the F-S transition region itself. In fact, none of the existing three- or four-parameter viscosity models in literature is capable of capturing $\eta(T)$ for F-S transition liquids across the full range of temperatures. Hence, there is a great need to develop a generalized viscosity model capable of capturing the dynamics of F-S liquids accurately.

We now propose a new viscosity model for F-S liquids based on a simple extension of the MYEGA expression in Eq. (2), which is derived based on a combination of the Adam–Gibbs equation[30] and the notion of temperature-dependent constraints.[5,31,32] Whereas the three-parameter form of Eq. (2) is obtained by assuming one dominant floppy-to-rigid transition as the liquid is cooled toward the glass transition, the anomalous F-S behavior can be captured using two constraint onset temperatures. With this approach, a generalized MYEGA expression can be written as

$$\log \eta = \log \eta_\infty + \frac{B}{T\left[w_1 \exp\left(-\frac{C_1}{T}\right) + w_2 \exp\left(-\frac{C_2}{T}\right)\right]}. \tag{6}$$

Physically, C_1 and C_2 correspond to two constraint onsets at which different structural mechanisms (weighted by w_1 and w_2, respectively) induce floppy-to-rigid transitions. For F-S transition liquids, these correspond to two different mechanisms controlling the dynamics in the fragile and strong regimes. Defining normalized weighting factors $W_1 = w_1/B$ and $W_2 = w_2/B$, Eq. (6) reduces to a five-parameter form

$$\log \eta = \log \eta_\infty + \frac{1}{T\left[W_1 \exp\left(-\frac{C_1}{T}\right) + W_2 \exp\left(-\frac{C_2}{T}\right)\right]}. \tag{7}$$

Please note that the standard three-parameter MYEGA expression of Eq. (7) is recovered when $C_1 = C_2$. This means that Eq. (7) is a generalized model describing the dynamic behavior of both F-S and non-F-S liquids. The two additional parameters are required to model the high temperature fragility and the F-S crossover temperature. Figure 3 shows fits of Eq. (7) to the viscosity data of $La_{55}Al_{25}Ni_{20}$ and $La_{55}Al_{25}Ni_{15}Cu_5$. By using a second constraint onset mechanism, Eq. (7) is able to capture the full range of viscosities, including both the high and low temperature ends, as well as the F-S transition region.

Table II lists the optimized parameter values of Eq. (7) for all F-S liquids under study. Here we note a clear separation of the parameters into two terms that dominate the dynamics in either the high temperature (i.e., fragile) or low

TABLE II. Optimized viscosity parameters using the extended MYEGA model of Eq. (7).

Composition	$\log \eta_\infty$ (Pa s)	W_1	C_1	W_2	C_2
$Gd_{55}Al_{25}Co_{20}$	−2.49	7966	13 188	0.000 27	503
$Gd_{55}Al_{25}Ni_{10}Co_{10}$	−2.39	3078	12 327	0.000 28	500
$Pr_{55}Ni_{25}Al_{20}$	−3.03	5180	12 674	0.000 32	412
$Sm_{55}Al_{25}Co_{10}Ni_{10}$	−2.24	517	10 707	0.000 33	524
$Sm_{50}Al_{30}Co_{20}$	−2.35	1526	13 516	0.000 28	498
$Sm_{55}Al_{25}Co_{10}Cu_{10}$	−2.60	1205	13 166	0.000 32	482
$La_{55}Al_{25}Ni_{20}$	−2.89	4715	11 032	0.000 47	609
$La_{55}Al_{25}Ni_{15}Cu_5$	−3.13	6993	13 414	0.000 48	587
$La_{55}Al_{25}Ni_5Cu_{15}$	−3.11	1806	10 829	0.000 54	600
$Al_{87}Co_8Ce_5$	−2.59	559	10 683	0.000 33	558
$Ce_{55}Al_{45}$	−2.89	1181	10 628	0.000 39	630

temperature (i.e., strong) regimes. This is illustrated in Fig. 4 for $La_{55}Al_{25}Ni_{20}$ and $La_{55}Al_{25}Ni_{15}Cu_5$, where we show that using a single exponential in Eq. (7) can capture either the fragile or the strong regime separately, but both terms are required to reproduce the F-S transition region. Please note that, plotted separately, the fragile and strong liquid phases would exhibit two independent glass transition temperatures.[33] As is evident in Fig. 4, the fragile phase would exhibit a much higher T_g compared to the strong phase. However, as the fragile liquid is cooled, the fragile-to-strong transition intervenes, effectively mitigating the increase in viscosity with decreasing temperature. Since this fragile-to-strong transition occurs at viscosities well below the T_g of the fragile phase, the actual T_g exhibited by the equilibrium liquid corresponds to that of the strong liquid. It is this equilibrium (or standard) T_g that we use for normalization of the temperature axis in all of the figures.[22] It should be mentioned that the optimized viscosity parameters, especially W_1, are sensitive to the number of the data points used for fitting. To obtain the optimized viscosity parameters that can accurately describe the F-S transition, it is essential to acquire sufficient viscosity data points in both the high and low temperature regions.

Physically, the fragile term in Eq. (7) (dominant at high temperatures), corresponds to a relaxation mechanism having both a high activation enthalpy and a high transition point entropy. Conversely, the strong term (dominant at low temperatures), results from a comparatively low activation enthalpy and low transition point entropy. This relationship among fragility, activation enthalpy, and entropy has been analyzed in detail by Mauro and Loucks[34] within the energy landscape framework. Based on this discussion, it is apparent that a reverse strong-to-fragile transition is not a physically realistic scenario, since the higher entropy mechanisms will always be more dominant at higher temperatures leading to higher values of fragility. Hence, the F-S transition parameter f of Eq. (5) can never be less than unity.

The entropic nature of the F-S transition also explains the wide range of values in Table II for C_1 and W_1 of the fragile phase at high temperatures versus C_2 and W_2 of the strong phase at low temperatures. The higher value of $C_1 > C_2$ is indicative of a higher activation enthalpy for the dynamics in the fragile phase. However, at high temperatures this is more than compensated by the greater $W_1 > W_2$, which indicates a much greater number of transition paths (i.e., transition point entropy) for the fragile phase. In the energy landscape framework, the system samples phase space with deeper enthalpy wells but a much greater number of escape pathways (the number of which can vary by orders of magnitude[34]). In contrast, the strong phase is characterized by shallower enthalpy wells with a fewer number of transition pathways. Please note that this type of competition between entropy and enthalpy is essential for the existence of a fragile-to-strong transition. In the absence of such competition, it is impossible to have such characteristically different scaling of dynamics at different temperatures.

Since the F-S transition with $f > 1$ is found to be a general feature in the MGFLs, the next question relates to the chemical origin of the F-S transition in the MGFLs. Based on recent findings in various glasses,[20,35–38] it can be inferred that the F-S transition could be associated with a polyamorphic transition. For example, a previous study has demonstrated a pressure-induced transition between two distinct amorphous polymorphs in a $Ce_{55}Al_{45}$ glassy metal, i.e., a crossover from a low-density glass to a high-density glass.[35] The large density difference observed between the two polyamorphs is attributed to their different electronic and short-range atomic structures, in particular, to the Ce–Ce bond shortening associated with the 4-f electron delocalization.[35] The pressure-induced bond shortening could also occur in the glasses studied in this work, since these glasses contain the rare earth elements Gd, Pr, and Sm that exhibit a 4-f delocalization effect. The $Ce_{55}Al_{45}$ glassy metal, in which the polyamorphic transition was observed, exhibits a pronounced F-S transition, as shown in Fig. 2(b). As implied in the previous work,[16,19] glasses exhibiting a pressure-induced polyamorphic transition also display a F-S transition in dynamics, implying that the structural arrangement in the MGFLs at $T > T_{liq}$ is significantly different from that of the corresponding glasses and/or the supercooled liquids near T_g. In other words, the F-S transition is a dynamic transition accompanied by the occurrence of polyamorphism. This may be the chemical basis for the presence of two constraint hardening mechanisms as in Eq. (7). The phenomenon of polyamorphism has also been observed and clarified in numerous amorphous materials such as water,[36]

yttria-alumina,[37,38] and chalcogenides.[39] It should be pointed out that although the polyamorphic transition in the vitreous state occurs gradually, the transition in supercooled liquids is abrupt and reversible.[38] According to a recent study[20] an order-disorder transition occurs in a Zr-based system when it is heated from a glass through the supercooled liquid region to the liquid state above T_{liq}. It has been shown that bulk glassy metals often exhibit an entropy just barely higher than that of the crystal.[40] In the strong high-viscosity liquid, both short-range and medium-range order must exist, which can be destroyed by increasing the temperature leading to a much more fragile liquid with higher configurational entropy. In contrast to most oxide systems, where the order-disorder transition occurs gradually with increasing temperature, the MGFLs exhibit an abrupt transition under an applied pressure. The medium-range order in glassy metals is formed by placing the icosahedral short-range ordered clusters on icosahedral lattice.[41]

Moreover, it has been found that the F-S transition is a dynamic anomaly coupled with a thermodynamic anomaly, e.g., the existence of an isochoric heat capacity (C_v) maximum in the middle of the F-S transition region.[16] The C_v maximum implies a rapid but continuous crossover in the thermodynamic properties of the liquid. To establish whether or not such a thermodynamic transition also occurs in the MGFLs, it would be essential to measure the heat capacity data of MGFLs both in the glass transition region and in the high T region above T_{liq}. It is known that the configurational relaxation is more cooperative in strong systems than in fragile systems. Therefore, we postulate that there should be a jump in the cooperative degree of structural relaxation during the F-S transition. According to Angell,[4] there are two kinds of F-S transitions: one with an excess heat capacity (ΔC_p) peak between T_g and T_m and another with a ΔC_p peak above T_m. The former one is often linked to poor glass-formers, e.g., water, and amorphous solids such as Si and Ge. The latter F-S transition is associated with a high glass-forming ability, such as in BeF_2 and SiO_2. Thus, the relatively poor glass-forming ability of MGFLs indicates that the F-S transition in these systems should be accompanied by a ΔC_p peak between T_g and T_m. Whereas silica and water are anomalous among other oxides, the F-S transition appears to be a general phenomenon in MGFLs. The MGFLs also share another property with water, viz., a low liquidus viscosity of approximately 10^{-3} Pa s, leading to rather poor glass-forming ability.

V. CONCLUSIONS

All of the MGFLs under study exhibit a striking fragile-to-strong transition. The extent of the fragile-to-strong transition can be quantified by the transition factor f, which depends on the chemical nature of MGFLs. Our observations imply that the fragile-to-strong (F-S) transition might be a general dynamic feature of all MGFLs. We have proposed a new viscosity model for F-S liquids with two relaxation mechanisms. Our findings imply that the F-S transition is intrinsic to strong liquid systems as a relaxation mode of higher entropy and higher activation barrier becomes dominant at some high temperatures for these systems.

ACKNOWLEDGMENTS

We are grateful for the financial support from the National Basic Research Program of China (973 Program) (Contract No. 2007CB613901), the National Natural Science Foundation of China (Grant Nos. 50801041, 50631010, and 50471052), the Research Fund for the Doctoral Program of Higher Education of China (Grant No. 200804221041), and the Danish Research Council (Grant No. 274-07-0493). We also thank C. A. Angell for valuable discussions, X. F. Bian for technical support, and M. M. Smedskjaer for careful review of our manuscript.

[1] C. A. Angell, Chem. Rev. (Washington, D.C.) **102**, 2627 (2002).
[2] L. M. Martinez and C. A. Angell, Nature (London) **410**, 663 (2001).
[3] C. A. Angell, Science **267**, 1924 (1995).
[4] C. A. Angell, J. Non-Cryst. Solids **354**, 4703 (2008).
[5] J. C. Mauro, Y. Z. Yue, A. J. Ellison, P. K. Gupta, and D. C. Allan, Proc. Natl. Acad. Sci. U.S.A. **106**, 19780 (2009).
[6] Z. P. Lu, Y. Li, and C. T. Liu, J. Appl. Phys. **93**, 286 (2003).
[7] C. T. Moynihan, Rev. Mineral. **32**, 1 (1995).
[8] Y. Z. Yue, R. von der Ohe, and S. L. Jensen, J. Chem. Phys. **120**, 8053 (2004); **121**, 11508 (2004).
[9] K. Ito, C. T. Moynihan, and C. A. Angell, Nature (London) **398**, 492 (1999).
[10] C. A. Angell, J. Phys. Chem. **97**, 6339 (1993).
[11] E. A. Jagla, J. Phys.: Condens. Matter **11**, 10251 (1999).
[12] H. Tanaka, J. Phys.: Condens. Matter **15**, L703 (2003).
[13] L. Liu, S. H. Chen, A. Faraone, C. W. Yen, and C. Y. Mou, Phys. Rev. Lett. **95**, 117802 (2005).
[14] J. Hedström, J. Swenson, R. Bergman, H. Jansson, and S. Kittaka, Eur. Phys. J. Spec. Top. **141**, 53 (2007).
[15] J. L. Barrat, J. Badro, and P. Gillet, Mol. Simul. **20**, 17 (1997).
[16] I. Saika-Voivod, F. Sciortino, and P. H. Poole, Nature (London) **412**, 514 (2001).
[17] M. Hemmati, C. T. Moynihan, and C. A. Angell, J. Chem. Phys. **115**, 6663 (2001).
[18] B. W. H. van Beest, G. J. Kramer, and R. A. van Santen, Phys. Rev. Lett. **64**, 1955 (1990).
[19] I. Saika-Voivod, F. Sciortino, and P. H. Poole, Phys. Rev. E **69**, 041503 (2004).
[20] C. Way, P. Wadhwa, and R. Busch, Acta Mater. **55**, 2977 (2007).
[21] L. Hu, X. F. Bian, X. B. Qin, Y. Z. Yue, Y. Zhao, and C. D. Wang, J. Phys. Chem. B **110**, 21950 (2006).
[22] Y. Z. Yue, J. Non-Cryst. Solids **355**, 737 (2009).
[23] J. C. Mauro, D. C. Allan, and M. Potuzak, Phys. Rev. B **80**, 094204 (2009).
[24] Q. G. Meng, S. G. Zhang, J. G. Li, and X. F. Bian, J. Alloys Compd. **431**, 191 (2007).
[25] R. Roscoe, Proc. Phys. Soc. London **72**, 576 (1958).
[26] J. Guo, X. F. Bian, X. L. Li, and C. D. Wang, Sci. China, Ser. G **51**, 387 (2008).
[27] J. Guo, "Study of glass-forming ability and liquid fragility of bulk metallic glasses," Ph.D. thesis, Shandong University, China, 2008.
[28] X. F. Bian, B. A. Sun, L. N. Hu, and Y. B. Jia, Phys. Lett. A **335**, 61 (2005).
[29] T. Komatsu, J. Non-Cryst. Solids **185**, 199 (1995).
[30] G. Adam and J. H. Gibbs, J. Chem. Phys. **43**, 139 (1965).
[31] P. K. Gupta and J. C. Mauro, J. Chem. Phys. **130**, 094503 (2009).
[32] J. C. Mauro, P. K. Gupta, and R. J. Loucks, J. Chem. Phys. **130**, 234503 (2009).
[33] G. N. Greaves, F. Meneau, A. Sapelkin, L. M. Colyer, I. ap Gwynn, S. Wade, and G. Sankar, Nature Mater. **2**, 622 (2003).
[34] J. C. Mauro and R. J. Loucks, Phys. Rev. E **78**, 021502 (2008).
[35] H. W. Sheng, H. Z. Liu, Y. Q. Cheng, J. Wen, P. L. Lee, W. K. Luo, S. D.

Shastri, and E. Ma, Nature Mater. **6**, 192 (2007).
[36] O. Mishima, L. D. Calvert, and E. Whalley, Nature (London) **314**, 76 (1985).
[37] P. F. McMillan, J. Mater. Chem. **14**, 1506 (2004).
[38] G. N. Greaves, M. C. Wilding, S. Fearn, D. Langstaff, F. Kargl, S. Cox, Q. Vu Van, O. Majerus, C. J. Benmore, R. Weber, C. M. Martin, and L. Hennet, Science **322**, 566 (2008).
[39] S. Sen, S. Gaudio, B. G. Aitken, and C. E. Lesher, Phys. Rev. Lett. **97**, 025504 (2006).
[40] A. L. Greer, Mater. Today **12**, 14 (2009).
[41] H. W. Sheng, W. K. Luo, F. M. Alamgir, J. M. Bai, and E. Ma, Nature (London) **439**, 419 (2006).

Reprint 13-2: Thermodynamic Anomaly of the Sub-Tg Relaxation in Hyperquenched Metallic Glasses

L. Hu, C. Zhou, C. Zhang, and Y. Yue

J. Chem. Phys., 138, 174508 (2013)

Thermodynamic anomaly of the sub-T_g relaxation in hyperquenched metallic glasses

Lina Hu,[1,a)] Chao Zhou,[1] Chunzhi Zhang,[2] and Yuanzheng Yue[1,3]
[1]*Key Laboratory of Liquid Structural Evolution and Processing of Materials (Ministry of Education), Shandong University, Jinan 250061, China*
[2]*School of Materials Science and Engineering, Shandong University of Science and Technology, Qingdao 266590, China*
[3]*Section of Chemistry, Aalborg University, DK-9000 Aalborg, Denmark*

(Received 18 January 2013; accepted 15 April 2013; published online 7 May 2013)

Recently, we observed an unusual non-monotonic glass relaxation phenomenon, i.e., the three-step sub-T_g relaxation in hyperquenched CuZrAl glass ribbons [L. N. Hu and Y. Z. Yue, Appl. Phys. Lett. **98**, 081904 (2011)]. In the present work, we reveal the origin of this abnormal behavior by studying the cooling rate dependence of the sub-T_g enthalpy relaxation in two metallic glasses. For the $Cu_{46}Zr_{46}Al_8$ glass ribbons the sub-T_g enthalpy relaxation pattern exhibits a three-step trend with the annealing temperature only when the ribbons are fabricated below a critical cooling rate. For the $La_{55}Al_{25}Ni_{20}$ glass ribbons the activation energy for the onset of the sub-T_g enthalpy relaxation also varies non-monotonically with the cooling rate of fabrication. These abnormal relaxation phenomena are explained in terms of the competition between the low and the high temperature clusters during the fragile-to-strong transition. By comparisons of chemical heterogeneity between $Cu_{46}Zr_{46}Al_8$ and $La_{55}Al_{25}Ni_{20}$, we predict that the abnormal relaxation behavior could be a general feature for the HQ metallic glasses. © *2013 AIP Publishing LLC*. [http://dx.doi.org/10.1063/1.4803136]

I. INTRODUCTION

Part of the difficulty in understanding the nature of metallic glass-forming liquids (MGFLs) is due to the crystallization problem in the temperature range, i.e., in the "no-man's land" prior to the glass formation upon cooling.[1] To overcome this difficulty, the hyperquenching (HQ) strategy is often used to arrest the structure of the supercooled liquid at a temperature well above the glass transition temperature, and subsequently annealing is done to let the arrested structure relax again in a controlled manner.[2,3] By comparisons in thermal scanning curves between bulk and HQ amorphous thin films, the intermediate martensitic transformation without phase separation has been detected in the shape memory alloy with a composition of $Zr_{50.59}Cu_{29.56}Ni_{19.85}$ (at.%).[4] Similarly, using the hyperquenching-annealing-calorimetric scanning approach, it has been found that the slow β relaxation also occurs in MGFLs, which has higher motion frequencies than the α relaxation.[5] The relaxation studies of the HQ glasses during reheating are also helpful for understanding the "liquid landscape."[6] Such studies provide access to some particular regions, where properties or relaxation mechanisms in supercooled liquids vary on very short time scales above T_g, e.g., to the crossover region of the mode coupling theory[7,8] and the well-known merging region of the α and slow β relaxations.[5,9]

In previous studies, it has already been known that the sub-T_g enthalpy relaxation pattern (ERP) of the HQ glass ribbons (e.g., FeNiP, AlNiCe, CuZr) is featured by a monotonic increase in the onset temperature T_{onset} with increasing the annealing temperature T_a.[10–13] This monotonic tendency in thermodynamics is expected since increasing T_a leads to the release of more excess enthalpy in HQ glass ribbons to reach lower energy states and become more stable. Our recent work, however, observed a different relaxation pattern, i.e., the three-step sub-T_g relaxation in HQ CuZrAl glass ribbons.[14] Interestingly, in a certain temperature region, T_{onset} and H_{anneal} decrease unexpectedly with the increase in T_a. This abnormal three-step relaxation pattern was seldom reported in metallic glass ribbons investigated previously. Now the questions arise: Is this non-monotonic three-step relaxation related to thermal history? Or is it only specific for $Cu_{48}Zr_{48}Al_4$ and $Cu_{45}Zr_{45}Al_{10}$ metallic glasses? We noticed that in previous studies the quenching conditions of the HQ glass ribbons were often ignored. How does the cooling rate of fabrication influence the sub-T_g ERP of HQ glass ribbons? How does such influence depend on the chemical nature of materials? The answers to these questions will be crucial for clarifying the features of thermodynamic evolution of the MGFLs approaching the "no-man's" land, then for further understanding their dynamic and thermodynamic properties in the supercooled liquid region.

It should be mentioned that, in this unstable region, some abnormal changes could occur, e.g., the fragile-to-strong (F-S) transition.[15,16] Both the experiments on viscosity and the recent simulation work have indicated that the F-S transition takes place in MGFLs during cooling towards the glassy state.[17–20] Although the possible thermodynamic evidence (such as enthalpy or entropy) of the dynamic F-S transition has been proposed,[21] systematic studies for such relation are still lacking due to the high tendency of MGFLs to

a)Author to whom correspondence should be addressed. Electronic mail: hulina0850@mail.sdu.edu.cn

crystallization during cooling. In this work, we attempt to find out whether there is a relation between the abnormal three-step sub-T_g relaxation and the dynamic F-S transition in MGFLs. We explore the sub-T_g ERP of fresh $Cu_{46}Zr_{46}Al_8$ glass ribbons with different fictive temperatures. We also examine whether the abnormal sub-T_g ERP occurs in other metallic glass ribbons. By considering the abnormal evolution of the activation energy during slowing down of MGFLs, we provide the thermodynamic evidence for the dynamic F-S transition. Finally, we discuss the effect of the chemical features of metallic glasses on the sub-T_g ERP.

II. EXPERIMENTAL PROCEDURES

The $Cu_{46}Zr_{46}Al_8$ and $La_{55}Al_{25}Ni_{20}$ HQ glass ribbons were selected as the objects of this study. According to our previous work,[14] the $Cu_{46}Zr_{46}Al_8$ HQ glass ribbons could exhibit the three-step sub-T_g ERP. This glass system was used to study the influence of the cooling rate of fabrication on the abnormal ERP. As a comparison, $La_{55}Al_{25}Ni_{20}$ HQ glass ribbons were investigated by changing the cooling rate in order to find the origin of the abnormal thermodynamic evolution. The master alloys were prepared by melting the elemental metals with purities ranging from 99.9%–99.999% in an arc furnace under argon atmosphere. The HQ glass ribbons used for this study were fabricated by the single copper roller melt-spinning technique under high-purity argon atmosphere. The master alloys were re-melted using the high-frequency induction technique and rapidly solidified into continuous ribbons at different circumferential velocities. Since the spinning velocity is proportional to the cooling rate that the glasses undergo, it is used as a measure of the cooling rate hereafter.

The HQ glass ribbons were annealed in nitrogen gas (99.9%) at various temperatures below T_g for 1 h. To measure the enthalpy response of glass ribbons, the calorimetric measurements were performed using the Netzsch DSC404 calorimeter with high-purity standard platinum pans under a constant flow of high-purity argon, using pure indium (99.999% mass percent) and zinc (99.999% mass percent) standards and a sample mass of 20 ± 0.5 mg. All the DSC measurements were conducted in a flowing (30 cm^3/min) nitrogen gas. To obtain the standard glasses, all the HQ ribbons were held at 303 K for 5 min and were upscanned to a temperature slightly above the glass transition temperature at 20 K/min and then cooled at 20 K/min. The standard glasses used in the present work refer to the samples subjected to the standard cooling rate of 20 K/min. The T_g values of the standard $Cu_{46}Zr_{46}Al_8$ and $La_{55}Al_{25}Ni_{20}$ samples are 695 and 473 K, respectively. To determine the heat capacity curve of a sample, both baseline and reference sample (here sapphire) were measured.

For the HQ samples (fresh or annealed), the fictive temperature T_f is an important value, since it is the temperature at which a supercooled liquid is frozen in during cooling.[22,23] Figure 1 shows the isobaric heat capacity C_p curves of an annealed HQ sample (C_{p1}) and the standard glass (C_{p2}) for $Cu_{46}Zr_{46}Al_8$, from which the T_f value can be determined. According to the enthalpy-matching method,[23] the value of T_f of the annealed sample can be determined by making area A equal to B. The area A means the remnant excess enthalpy of the glass ribbons relative to the standard glasses, denoted by H_{rem}. It can be expected that a high cooling rate will cause larger A, and hence a higher T_f. During the annealing procedure, the T_f of the glass ribbons decreases due to the release of the remnant excess enthalpy of the sample, i.e., due to the decrease in the area A. For the standard glasses, the T_f and the T_g values are expected to be equal. The detailed calculation of T_f has been described in Refs. 9 and 23.

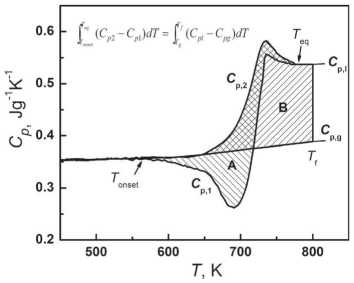

FIG. 1. Isobaric heat capacity (C_p) versus temperature (T) for the annealed $Cu_{46}Zr_{46}Al_8$ glass ribbons (C_{p1}) and the standard glasses (C_{p2}). C_{pl} and C_{pg} are, respectively, the liquid and the glass heat capacities. T_{onset} is the temperature, at which the release of the remnant excess energy starts, and T_{eq} is the temperature, at which $C_{p1} = C_{p2}$. The shadow areas (A and B) are used to determine T_f using the enthalpy-matching method.

The activation energy (E_{onset}) for the onset of the excess enthalpy release during thermal scanning for the fresh glass ribbons can be calculated from the equation[24]

$$\ln \Phi = -E_{onset}/RT_{onset,\Phi} + Const, \qquad (1)$$

where R is the gas constant and Φ is the scanning heating rate. $T_{onset,\Phi}$, as shown in Fig. 1, is the onset temperature of releasing the remnant excess enthalpy of the quench during heating by Φ, i.e., the temperature where DSC trace changes from "going up" to "going down." For each measurement to determine the value of E_{onset}, the fresh glass ribbons were directly heated through the glass transition region at Φ of 5, 10, 20, 30, 40 K/min, respectively. The largest measure tolerance was 1 K. Therefore, the value of E_{onset} for each sample was determined from the slope of $\ln\Phi$ vs. $1/T_{onset,\Phi}$.

All the ribbons were measured using the x-ray diffraction (XRD) method under the conditions: Cu Kα radiation, graphite monochromator, 40 kV, 100 mA, the scattering angle 2θ in the range 5°–80°, and the temperature error of ±2 K. The XRD results indicate that the sub-T_g annealing did not change the amorphous nature of the glass ribbons.

III. RESULTS AND DISCUSSIONS

A. The evolution of sub-T_g ERP with cooling rate for $Cu_{46}Zr_{46}Al_8$

Figure 2 shows the C_p curves for the HQ $Cu_{46}Zr_{46}Al_8$ glass ribbons cooled at 49 m/s and subsequently annealed at different temperatures (T_a) well below T_g for 1 h. A distinct

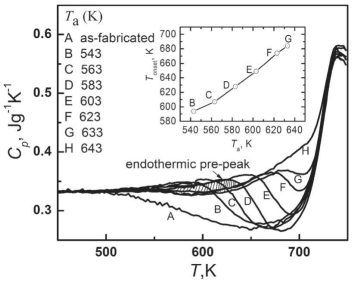

FIG. 2. The isobaric heat capacity (C_p) versus temperature (T) for the $Cu_{46}Zr_{46}Al_8$ glass ribbons cooled at 49 m/s, exhibiting the effect of the annealing temperature (T_a) on the sub-T_g relaxation pattern (the energy release behavior) for the duration of 1 h. The shaded area is the endothermic pre-peak of curve D relative to curve H.

exothermic peak is observed in each of the curves when T_a is well below 633 K, indicating that the remnant excess enthalpy in the HQ samples relative to standard glasses is released during reheating. This energy recovery is followed by the glass transition peak. The presence of these two peaks (exothermic and endothermic) in Fig. 2 is the same as those observed in the normal HQ glasses reported previously.[10–13] It is noticed that the value of T_{onset} for each C_p curve shifts to the high temperature with increasing T_a, exhibiting a positive monotonic trend (shown in the inset). T_{onset} is the temperature, at which some structural domains in glass ribbons start to lose their excess potential energy. Thus, the $T_{onset} \sim T_a$ relation in Fig. 2 could be attributed to the fact that a viscous slowing down is caused by an increase in the stability of microstructures (or in the correlation length) upon cooling towards T_g. The sub-T_g ERP of the $Cu_{46}Zr_{46}Al_8$ sample cooled at 49 m/s agrees with that observed in the "normal" HQ glass ribbons,[5,10–13] whereas it contrasts to the three-step ERP observed in the HQ $Cu_{48}Zr_{48}Al_4$ and $Cu_{45}Zr_{45}Al_{10}$ glass ribbons.[14]

When the cooling rate is decreased from 49 to 35, 25, and 17 m/s, the ERPs of the HQ $Cu_{46}Zr_{46}Al_8$ samples vary as shown in Figs. 3(a)–3(c), respectively. The anomaly of the sub-T_g relaxation behavior is reflected by the dashed curves in Fig. 3. For $T_a \leq 583$ K (curves A–D in Fig. 3(a)), T_{onset} increases monotonically with T_a. The former is about 40–50 K higher than the latter. But when T_a is increased from 583 to 603 K (curves D–E), T_{onset} decreases abruptly down to 590 K. For $T_a \geq 603$ K, T_{onset} increases again with T_a (curves F–I). Such a three-step relaxation pattern, i.e., the breakdown of the monotonic trend, is also seen in Figs. 3(b) and 3(c). This suggests that structural changes in the HQ glass ribbons take place during annealing, which results in energy release (i.e., enthalpy recovery) from some structural domains during the subsequent DSC upscanning. The breakdown of the monotonic trend can be characterized by the critical annealing temperature $T_{a,c}$, at which the $T_a \sim T_{onset}$ relation varies from a positive to a negative trend. In the insets of Fig. 3, it is seen that $T_{a,c}$ is the same (about 583 K) for both the 35 K/s sample and the 25 m/s sample, and it is about 603 K for the 17 m/s sample. This indicates that the $T_{a,c}$ value is only slightly dependent on the T_f of the fresh glass ribbons.

In Fig. 2, an endothermic pre-peak appears for each curve (A–E) relative to curve H (see the shaded area of curve D). However, there are no endothermic pre-peaks on both curve E in Figs. 3(a) and 3(b) and curve F in Fig. 3(c). The origin of the endothermic pre-peaks has been discussed in literature.[12,25,26] According to it, the anomaly of the dashed curves indicates that during annealing some microstructures with fast relaxation exhibit the tendency to reach high energy states relative to the rest of glass, and then return to the lower energy states during DSC upscan. Thus, the loss of the endothermic pre-peak of the dashed curves accords with what the abnormal $T_a \sim T_{onset}$ relation suggests.

By comparisons between Figs. 2 and 3, it is clear that the cooling rate has a strong impact on the sub-T_g ERP of the fresh glass ribbons. When the cooling rate is decreased from 49 to 17–35 m/s, the $H_{rem} \sim T_a$ relation becomes a non-monotonic one. In order to further reveal the anomaly of the sub-T_g relaxation, we explore the T_f dependence of the remnant excess enthalpy of the samples, H_{rem}, for the starting material cooled at 49 and 25 m/s (Fig. 4). It should be noted that the T_f in Fig. 4 refers to the fictive temperature

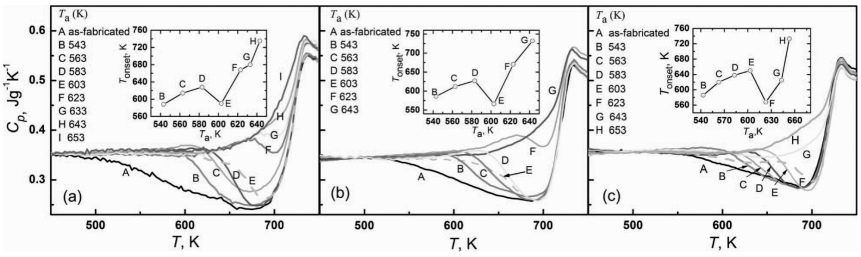

FIG. 3. The isobaric heat capacity (C_p) versus temperature (T) for the three HQ $Cu_{46}Zr_{46}Al_8$ samples annealed at different temperatures (T_a) below T_g for 1 h. The three fresh samples were hyperquenched at (a) 35 m/s, (b) 25 m/s, and (c) 17 m/s, respectively. Insets: the relationship between the onset temperature of the exothermic peak (T_{onset}) and the annealing temperature (T_a). For the curves without an exothermic peak, the peak temperature of the glass transition is used as T_{onset} in the insets.

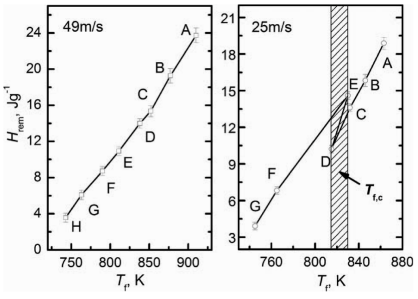

FIG. 4. T_f dependence of the remnant excess enthalpy, H_{rem}, for the $Cu_{46}Zr_{46}Al_8$ samples cooled at 49 m/s and 25 m/s, respectively. The capitals near the curves correspond to those in Figs. 2 and 3(b), respectively. Shaded area: the critical fictive temperature range ($T_{f,c}$), in which the abnormal sub-T_g ERP occurs.

of both the fresh HQ and the annealed HQ samples, which was determined using the enthalpy-matching method.[23] For the 49 m/s sample, H_{rem} exhibits a monotonic increase with temperature as is generally expected. When the liquid structure of $Cu_{46}Zr_{46}Al_8$ is frozen in at 25 m/s, giving a T_f value of 863 K, the $H_{rem} \sim T_f$ relation is manifested as a three-step fashion. An abnormal increase in H_{rem} takes place in the 25 m/s sample in the critical fictive temperature range ($T_{f,c}$) between 815 and 828 K. This suggests that the microstructures in $Cu_{46}Zr_{46}Al_8$ supercooled liquids tend to be different between 910 and 863 K. The structural evolution for the supercooled $Cu_{46}Zr_{46}Al_8$ liquid at 863 K (i.e., at the T_f of the fresh sample cooled at 25 m/s) is discontinuous during cooling and this might be attributed to the first-order phase transition. The latter has been observed in a monoatomic ideal metallic glass former.[27] By using a molecular dynamics approach the discontinuous change of enthalpy with temperature has also been confirmed for the CuZr supercooled liquid, which involves the F-S transition.[19]

TABLE I. The $T_{onset,\Phi}$ values for the HQ glass ribbons cooled at different rates and the correlation factors representing the linear fitting quality of the relationship between $\ln\Phi$ and $1/T_{onset,\Phi}$ in Eq. (1).

Cooling rate	$T_{onset,\Phi} \pm 1$ K					Correlation factor
	5 K/min	10 K/min	20 K/min	30 K/min	40 K/min	
25 m/s	367	378	381	390	401	0.994
35 m/s	370	375	383	388	399	0.992
44 m/s	368	375	383	387	394	0.997

B. Evolution of sub-T_g ERP with cooling rate for $La_{55}Al_{25}Ni_{20}$

Figure 5 shows the release of the remnant excess enthalpy in the HQ samples relative to the standard sample during the DSC upscan, which is reflected by the exothermic peak prior to the glass transition peak. With increasing T_a, the exothermic peak tends to gradually diminish, leading to a decrease of T_f. The monotonic relation between H_{rem} and T_f is consistent with that between T_{onset} and T_a as shown in the inset of Fig. 5(a). However, the monotonic $T_{onset} \sim T_a$ relation is disrupted by sample E (annealed at 423 K) as shown in Figs. 5(b) and 5(c). It is noticed in Fig. 5(a) that there is a distinct endothermic pre-peak on curve E relative to curve F (for the standard glass). Such a pre-peak does not exist on curve E in Figs. 5(b) and 5(c). As has been discussed for $Cu_{46}Zr_{46}Al_8$ (see Fig. 3), the loss of the endothermic pre-peak hints the existence of the three-step relaxation pattern in the $La_{55}Al_{25}Ni_{20}$ samples cooled at 35 and 44 m/s. However, the three-step $H_{rem} \sim T_f$ relation is not observed in these samples.

To further probe the three-step $T_a \sim T_{onset}$ relation in the $La_{55}Al_{25}Ni_{20}$ HQ samples, we determine the activation energy E_{onset}, i.e., the energy barrier to be overcome for the energy release during thermal scanning. It is generally accepted that the increasing structural correlation length with high activation energy contributes to slowing down of the liquids upon cooling. This means that the more slowly cooled glass ribbons should have higher activation energy for structure relaxation during reheating. Table I shows the $T_{onset,\Phi}$ values of the fresh HQ glass ribbons cooled at different rates. According to

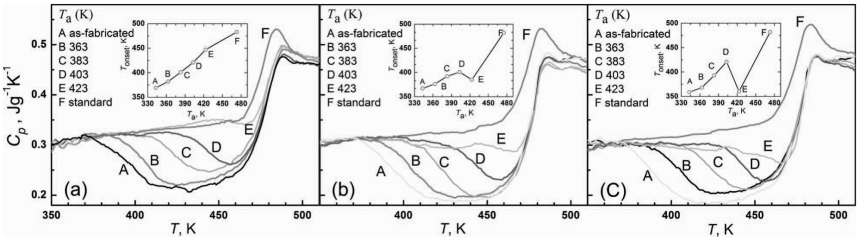

FIG. 5. The isobaric heat capacity (C_p) versus temperature (T) for the three HQ $La_{55}Al_{25}Ni_{20}$ samples annealed at different temperatures (T_a) below T_g for 1 h. The three fresh samples were hyperquenched at (a) 25 m/s, (b) 35 m/s, and (c) 44 m/s, respectively. Insets: the relationship between T_{onset} and T_a. For the curves without an exothermic peak, the peak temperature of the glass transition is used as T_{onset} in the insets.

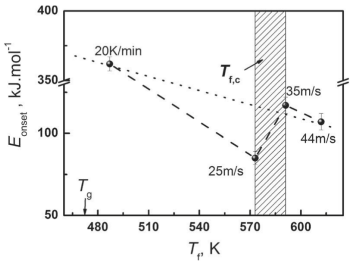

FIG. 6. The T_f dependence of the activation energy for the onset of the excess enthalpy release of the $La_{55}Al_{25}Ni_{20}$ sample relative to that of the standard glass. The activation energy for the standard sample is taken from Ref. 28. The dashed line is the guide for eyes. The dotted line represents the generally expected trend. Shaded area: the critical fictive temperature range ($T_{f,c}$), in which the abnormal decrease in E_{onset} occurs.

Eq. (1), the activation energy E_{onset} has been calculated and its relationship with T_f for the fresh glass ribbons is plotted in Fig. 6. It is shown that E_{onset} for the 44 m/s sample (T_f = 612 K) is 107 ± 5 kJ/mol, which is close to the activation energy for the slow β relaxation in $La_{55}Al_{25}Ni_{20}$.[5] This implies that the slow β relaxation has been frozen in at 44 m/s, and is dominant at the beginning of the energy release during the subsequent DSC scan. By reducing the cooling rate to 35 m/s, E_{onset} increases as expected with a decrease in T_f. However, the negative relationship between T_f and E_{onset} breaks down when the T_f value is below 591 K, and at T_f = 573 K, E_{onset} falls down to 87 kJ/mol. The abnormal decrease in the activation energy suggests that the structure in supercooled liquids around 573 K is less stable than that above 591 K, and an abrupt structural change occurs in the temperature region of 573–591 K. The sudden drop of the stability of the $La_{55}Al_{25}Ni_{20}$ supercooled liquid accords with the abnormal increase in H_{rem} with T_a observed in Fig. 4. The three-step trend shown in Fig. 6 verifies that the $La_{55}Al_{25}Ni_{20}$ glass has the same abnormal relaxation behavior as the $Cu_{46}Zr_{46}Al_8$ glass. Close to the $T_{f,c}$ range of 573–591 K (see the shaded area), where the abnormal relaxation behavior takes place in the $La_{55}Al_{25}Ni_{20}$ supercooled liquid, our previous x-ray diffraction experiments have revealed a distinct abnormal change of the pre-peak in the HQ $La_{55}Al_{25}Ni_{20}$ glasses.[29]

C. Correlation between the thermodynamic anomaly and the F-S transition

As shown in Figs. 4 and 6, for both the $Cu_{46}Zr_{46}Al_8$ and $La_{55}Al_{25}Ni_{20}$ glass ribbons there is a temperature region, in which the structure of the supercooled liquids abruptly changes. This change could be attributed to the F-S transition, which is found to be a general dynamic feature of MGFLs.[15,17–19] According to the previous work,[15,17–19] the F-S transition is due to the competition between two compositionally identical liquid phases that differ from each other only in density and structure.[17] Such a phenomenon, known as polyamorphism, can be induced by changing pressure or temperature. Considering that the clusters with the dense and efficient packing are the basis of the structural model of metallic systems, it is reasonable to use "clusters" to characterize the "liquid phase" of MGFLs. Therefore, both the discontinuous change in H_{rem} and the sudden drop of E_{onset} observed in the present work could be related to the temperature-induced transition from the high temperature (HT) to the low temperature (LT) clusters upon cooling. Besides, some of the LT clusters are even less stable than the HT clusters. This scenario could explain why the glass ribbons with different initial T_f values relax in different manners although they are annealed at the same temperature. For sample A cooled at 49 m/s (see Fig. 4), only the HT clusters are frozen in, which controls the subsequent relaxation during cooling. In contrast, for sample A cooled at 25 m/s (see Fig. 4), the LT clusters have strong tendency to form in the liquid, and then the following thermodynamic relaxations of the frozen glasses are attributed to choosing locally between HT and LT clusters. When the contribution of the LT clusters to the enthalpy relaxation becomes more dominant than that of the HT clusters, the critical $T_{f,c}$ range depicted by the shaded area in Figs. 4 and 6 will be present.

If the above scenario is correct, it would be expected that when the liquids are frozen in below $T_{f,c}$, the thermodynamic evolution of the fresh glasses will be mainly controlled by the evolution of the LT clusters, resulting in the disappearance of the abnormal three-step ERP. Figure 7 shows the sub-T_g ERP and the crystallization behaviors of the $Cu_{46}Zr_{46}Al_8$ glass ribbons cooled at 12 m/s, for which the T_f is about 804 K. In Fig. 7(a), it is observed that contrary to the three-step T_a dependence of T_{onset}, the T_{onset} increases monotonically with T_a, similar to the trend shown in Fig. 2. The glass transition peak is considerably affected by the sub-T_g annealing. This indicates that different from the HT clusters, the LT clusters frozen in glass ribbons are involved in the α relaxation (or glass transition peak). Moreover, two crystallization peaks have been observed in Fig. 7(b) in the 12 m/s sample. In contrast, for the 17–49 m/s samples, only one crystallization peak is present and almost independent on T_a (inset of Fig. 7(b)). All these facts imply that the clusters around 804 K are different in structural nature from those at higher temperatures. Another phenomenon worthy to be noticed is that in Fig. 7(b) the second crystallization peak, which is larger than the first peak, disappears when the annealing temperature reaches 633 K. Accompanied with this disappearance, the area of the first crystallization peak becomes larger, keeping the position unchanged. This phenomenon indicates the following two aspects. Firstly, some of the LT clusters that contribute to the second crystallization peak are unstable. Secondly, the LT clusters are more structurally heterogeneous than the HT clusters, since the two crystallization peaks, rather than one peak, have been observed in the glass ribbons at 12 m/s. This observation accords with the prediction by the two-order-parameter model and Jagla's model,[30–32] according to which the probability of locally choosing between two (or more) environments becomes larger at LT.

Although the difference in the liquid structures between HT and LT has been verified in Fig. 7, the detailed

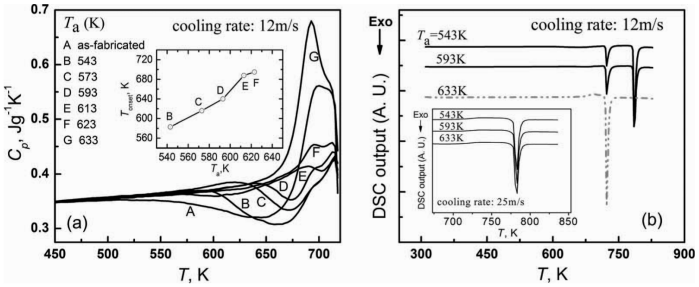

FIG. 7. The DSC curves for the HQ $Cu_{46}Zr_{46}Al_8$ glass ribbons quenched at 12 m/s. (a) Influence of the annealing temperature (T_a) for 1 h on the sub-T_g EPR. Inset: T_a dependence of the onset temperature (T_{onset}) of the sub-T_g ERP (on the C_p–T curves). (b) Influence of the annealing temperature (T_a) for 1 h on the crystallization peaks (on the DSC output–T curves). Inset: crystallization behavior of the samples quenched at 25 m/s for a comparison.

information concerning how the competition between the LT and HT clusters contribute to the abnormal relaxation process is still lacking. The energy landscape could be helpful for understanding this problem. It is known that the polyamorphism related to the F-S transition is attributed to visitations to distinct metabasins on the potential energy surface.[33] According to the minimalist landscape model that captures two-stage relaxation process, the three-step relaxation process observed in the present work might be obtained by embedding the metabasins inside a larger-scale metabasins.[34] The influence of the tradeoff between the entropic and enthalpic driving forces on relaxation processes has been revealed by using this minimalist landscape model. During cooling there is a probability for the system to be in the metabasin where the degeneracy is high, although this metabasin has higher inherent structure enthalpy than other metabasins.[34] This could be a reasonable scenario for explaining the non-monotonic T_f dependence of H_{rem} in Fig. 4. The different degeneracies of the metabasins might be one of the keys towards understanding the dynamics of glass forming systems.

Figure 8 shows the F-S transition of the $La_{55}Al_{25}Ni_{20}$ liquid in terms of the relationship between viscosity (η) and T_g/T. The two dashed curves were obtained by fitting the experimental viscosity data to the Mauro-Yue-Ellison-Gupta-Allan (MYEGA) equation for both low and high temperature regions, respectively.[35] The solid curve was obtained by fitting the viscosity data over the entire range of temperature to the following extended MYEGA equation:[17]

$$\log \eta = \log \eta_\infty + \frac{1}{T\left[W_1 \exp\left(-\frac{C_1}{T}\right) + W_2 \exp\left(-\frac{C_2}{T}\right)\right]}, \tag{2}$$

where C_1 and C_2 correspond to two constraint onsets reflecting different structural mechanisms (weighted by W_1 and W_2, respectively). Although the physical meaning of the parameters in Eq. (2) needs further clarification, the basic idea of the equation is related to two competing local structures: the HT clusters (i.e., fragile term) and the LT clusters (i.e., strong term). According to Eq. (2), the characteristic temperature, $T_{f\text{-}s}$, can be calculated from the equations:

$$W_1 \exp\left(-\frac{C_1}{T_{f-s}}\right) = W_2 \exp\left(-\frac{C_2}{T_{f-s}}\right),$$
$$T_{f-s} = \frac{C_1 - C_2}{\ln \frac{W_1}{W_2}}, \tag{3}$$

where the temperature $T_{f\text{-}s}$ is a quantitative measure to characterize the transition region, in which the fragile and the strong terms tend to be equal. As shown in the fragility plot (Fig. 8), the $T_g/T_{f\text{-}s}$ ratio is calculated to be 0.765, slightly smaller than $T_g/T_{f,c}$ (0.800–0.825), at which the activation energy E_{onset} drops as shown in Fig. 6. The difference between the two values agrees with the expected one, since, according to Fig. 8, the contribution from the LT clusters responsible for the strong term becomes dominant, rather than equivalent to that from the HT clusters, when $T_{f\text{-}s}$ decreases to $T_{f,c}$. This difference is also applicable to the $Cu_{46}Zr_{46}Al_8$ MGFLs. It has been found that for CuZr MGFLs there is a crossover of the temperature dependence of diffusion coefficient from

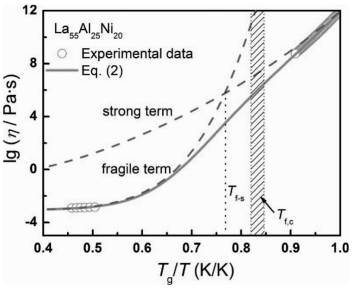

FIG. 8. Fragility diagram of the $La_{55}Al_{25}Ni_{20}$ liquids. Dashed lines: fits of the viscosity (η) data for both low and high temperature regions to the MYEGA equation.[35] Solid curve: fit of the viscosity data to Eq. (2). $T_{f\text{-}s}$ refers to the temperature where the fragile and the strong terms have an equal time scale during the F-S transition.

non-Arrhenius to Arrhenius behaviour when T_g/T is 0.769,[19] and an abnormal increase in the sub-T_g ERP is observed in the present work around 0.841 of $T_g/T_{f,c}$. Notice that the values of $T_{f,c}$ for both $Cu_{46}Zr_{46}Al_8$ (Fig. 4) and $La_{55}Al_{25}Ni_{20}$ (Fig. 6) are around $1.2T_g$, close to the temperature, at which the correlation length has an abnormal maximum found by the theoretical simulation work.[36,37] It was also reported that the unusual cluster expansion occurs around $1.2T_g$ in the PdNiCuP MGFLs during cooling,[38] which has been regarded as the evidence of the F-S transition.[39]

D. Influence of chemical heterogeneity on the three-step sub-T_g relaxation

As discussed above, the three-step relaxation pattern has the same origin as the dynamic F-S transition. This implies that like the F-S transition the abnormal ERP could also be a general feature of MGFLs. However, it is noticed that the distinct abnormal enthalpy increase with increasing the T_f, i.e., with decreasing the annealing degree, observed in $Cu_{46}Zr_{46}Al_8$ (Fig. 4) is not detected in $La_{55}Al_{25}Ni_{20}$. In this case, the drop in E_{onset} with decreasing the cooling rate, i.e., decreasing the T_f of the fresh sample (Fig. 6), implies the existence of the F-S transition. This phenomenon could be associated with the chemical or structural heterogeneities in supercooled liquids. As is known, the $Cu_{50}Zr_{50}$ liquid contains the Cu-centered clusters with the maximum packing efficiency, which are beneficial to GFA.[40] Adding a small amount of Al atoms into $Cu_{50}Zr_{50}$ can enhance the tendency to form Al-centered clusters in liquids.[41] Considering that the enthalpy of mixing between Cu and Al is only -1 kJ/mol, much smaller than that among other elements in $Cu_{46}Zr_{46}Al_8$, both types of clusters (Cu-centered and Al-centered) could competitively exist in $Cu_{46}Zr_{46}Al_8$ supercooled liquids. The existence of this kind of heterogeneity has been verified by the complicated formation of phases in the CuZrAl glass composites, as well as the existence of two glass transition processes.[42,43] The weak affinity between Cu-centered and Al-centered clusters, as well as the distinct difference between Cu and Al atoms, could contribute to a large enthalpy difference between the HT and the LT clusters. In accordance with it, Fig. 7(b) indicates that the LT clusters are more heterogeneous than the HT clusters. In the $La_{55}Al_{25}Ni_{20}$ supercooled liquid, the enthalpy of mixing among elements is rather negative (from -22 to -38), resulting in strong affinity among the elements. Taking the similarity between Al and Ni atoms into account (for example, both types of atoms can form symmetric metallic compounds), the chemical and structural properties of the Al-centered and the Ni-centered clusters should be similar.[29] This chemical or structural homogeneity in $La_{55}Al_{25}Ni_{20}$ leads to the similarity of enthalpy between the LT clusters and the HT clusters. As an evidence, $La_{55}Al_{25}Ni_{20}$ exhibits the smallest extent of the F-S transition among the investigated MGFLs.[17] The extent of the F-S transition, denoted by f, refers to the difference in fragility between the equilibrium (HT) and the supercooled (LT) liquids. This confirms the similarity between LT and HT clusters in $La_{55}Al_{25}Ni_{20}$, and therefore, the common chemical origin of the abnormal enthalpy change with T_f and the dynamic F-S transition in MGFLs.

IV. CONCLUSIONS

The influence of the cooling rate on the sub-T_g enthalpy relaxation behavior has been studied for the HQ $Cu_{46}Zr_{46}Al_8$ and $La_{55}Al_{25}Ni_{20}$ glass ribbons. Abnormal three-step relaxation pattern with respect to the fictive temperature has been detected in both types of glasses. This abnormal relaxation behavior is found to be a thermodynamic evidence of the dynamic fragile-to-strong transition, which is determined by the competitions between the LT and HT clusters in MGFLs. The abnormal relaxation behavior could be a general feature for the HQ metallic glasses, and its presentation is closely related to the chemical or structural heterogeneity in supercooled liquids. The hyperquenching-annealing strategy is proven to be a powerful tool providing the insights into the thermodynamic source of the F-S transition.

ACKNOWLEDGMENTS

This work was supported by National Natural Science Foundation of China (NNSFC) (Grant Nos. 50801041 and 51171090) and the Shandong Province Natural Science Foundation (Grant No. ZR2010EQ026).

[1] R. Busch, J. Schroers, and W. H. Wang, MRS Bull. **32**, 620 (2007).
[2] V. Velikov, S. Borick, and C. A. Angell, J. Phys. Chem. B **106**, 1069 (2002).
[3] C. A. Angell and L.-M. Wang, Biophys. Chem. **105**, 621 (2003).
[4] G. S. Firstov, Yu. N. Koval, J. Van Humbeeck, R. Portier, P. Vermaut, and P. Ochin, Mater. Sci. Eng. A **438–440**, 816 (2006).
[5] L. N. Hu and Y. Z. Yue, J. Phys. Chem. C **113**, 15001 (2009).
[6] L.-M. Wang, S. Borick, and C. A. Angell, J. Non-Cryst. Solids **353**, 3829 (2007).
[7] W. Götze, *Liquids, Freezing, and the Glass Transition* (NATO Advanced Study Institute, Amsterdam, 1989).
[8] U. Buchenau, J. Phys.: Condens. Matter **15**, S955 (2003).
[9] L. N. Hu and Y. Z. Yue, J. Phys. Chem. B **112**, 9053 (2008).
[10] A. Inoue, T. Masumoto, and H. S. Chen, J. Non-Cryst. Solids, **83**, 297 (1986).
[11] Y. H. Kim, A. Inoue, and T. Masumoto, J. Non-Cryst. Solids **127**, 233 (1991); G. P. Johari, J. Phys. Chem. B **107**, 9063 (2003).
[12] Y. Z. Yue and C. A. Angell, Nature (London) **427**, 717 (2004).
[13] A. Inoue, T. Zhang, and T. Masumoto, J. Non-Cryst. Solids **150**, 396 (1992).
[14] L. N. Hu and Y. Z. Yue, Appl. Phys. Lett. **98**, 081904 (2011).
[15] C. Way, P. Wadhwa, and R. Busch, Acta Mater. **55**, 2977 (2007).
[16] K. Ito, C. T. Moynihan, and C. A. Angell, Nature (London) **398**, 492 (1999); I. Saika-Voivod, F. Sciortino, and P. H. Poole, *ibid.* **412**, 514 (2001).
[17] C. Zhang, L. Hu, Y. Yue, and J. C. Mauro, J. Chem. Phys. **133**, 014508 (2010); C. Zhang, L. N. Hu, X. F. Bian, and Y. Z. Yue, Chin. Phys. Lett. **27**, 116401 (2010).
[18] Z. Evenson, T. Schmitt, M. Nicola, I. Gallino, and R. Busch, Acta Mater. **60**, 4712 (2012).
[19] K. N. Lad, N. Jakse, and A. Pasturel, J. Chem. Phys. **136**, 104509 (2012).
[20] A. Kushima, X. Lin, and S. Yip, J. Phys.: Condens. Matter **21**, 504104 (2009).
[21] C. A. Angell, J. Non-Cryst. Solids **354**, 4703 (2008).
[22] J. C. Mauro, D. C. Allan, and M. Potuzak, Phys. Rev. B **80**, 094204 (2009).
[23] Y. Z. Yue, J. deC. Christiansen, and S. L. Jensen, Chem. Phys. Lett. **357**, 20 (2002).
[24] C. T. Moynihan, J. Am. Ceram. Soc. **76**, 1081 (1993).
[25] H. Senapati and C. A. Angell, J. Non-Cryst. Solids **130**, 58 (1991).
[26] C. A. Angell, *Relaxations in Complex Systems* (National Technical Information Service, U.S. Department of Commerce, Springfield, 1985).

[27]M. Elenius, T. Oppelstrup, and M. Dzugutov, J. Chem. Phys. **133**, 174502 (2010).
[28]W. H. Wang, J. Appl. Phys. **110**, 053521 (2011).
[29]L. N. Hu, C. Z. Zhang, and Y. Z. Yue, Appl. Phys. Lett. **96**, 221908 (2010).
[30]H. Tanaka, J. Phys.: Condens. Matter **15**, L703 (2003).
[31]E. A. Jagla, J. Phys.: Condens. Matter **11**, 10251 (1999).
[32]L. M. Xu, S. V. Buldyrev, N. Giovambattista, and H. E. Stanley, Int. J. Mol. Sci. **11**, 5184 (2010).
[33]C. A. Angell, Science **267**, 1924 (1995).
[34]J. C. Mauro and M. M. Smedskjaer, Physica A **391**, 3446 (2012).
[35]J. C. Mauro, Y. Z. Yue, A. J. Ellison, P. K. Gupta, and D. C. Allan, Proc. Natl. Acad. Sci. U.S.A. **106**, 19780 (2009).
[36]W. Kob, S. Roldán-Vargas, and L. Berthier, Nat. Phys. **8**, 164 (2012).
[37]L. Berthier, G. Biroli, D. Coslovich, W. Kob, and C. Toninelli, Phys. Rev. E **86**, 031502 (2012).
[38]K. Georgarakis, D. V. Louzguine-Luzgin, J. Antonowicz, G. Vaughan, A. R. Yavari, T. Egami, and A. Inoue, Acta Mater. **59**, 708 (2011).
[39]Y. F. Guo, A. R. Yavari, and T. Zhang, J. Alloys Compd. **536**, S91 (2012).
[40]B. C. Lu, J. H. Yao, J. Xu, and Y. Li, Appl. Phys. Lett. **94**, 241913 (2009).
[41]H. Z. Fang, X. Hui, G. L. Chen, and Z. K. Liu, Appl. Phys. Lett. **94**, 091904 (2009).
[42]Y. Wu, H. Wang, H. H. Wu, Z. Y. Zhang, X. D. Hui, G. L. Chen, D. Ma, X. L. Wang, and Z. P. Lu, Acta Mater. **59**, 2928 (2011).
[43]D. V. Louzguine-luzgin, G. Xie, Q. Zhang, C. Suryanarayana, and A. Inoue, Metall. Mater. Trans. A **41**, 1664 (2010); E. S. Park, J. H. Na, and D. H. Kim, J. Appl. Phys. **108**, 053515 (2010).